DOI : 10.5050/KSNVE.2010.20.2.129

Position Tracking Control of Flexible Piezo-beam Considering Actuator Hysteresis

작동기 히스테리시스를 고려한 유연 피에조빔의 위치추적제어

Phuong-Bac Nguyen and Seung-Bok Choi
프엉박*·최 승 복†

(Received September 21, 2009 ; Accepted December 7, 2009)

Key Words : Hysteresis(히스테리시스), Piezoceramic Actuator(압전작동기), Preisach Model(프라이작 모델), Position Tracking Control(위치추적제어)

ABSTRACT

This paper presents a position tracking control of a flexible beam using the piezoelectric actuator. This is achieved by implementing both feedforward hysteretic compensator of the actuator and PID feedback controller. The Preisach model is adopted to develop the feedforward hysteretic compensator. In the design of the compensator, estimated displacement of the piezoceramic actuator is used based on the limiting triangle database that results from collecting data of the main reversal curve and the first order ascending curves. Experimental implementation is conducted for position tracking control and performance comparison is made between a PID feedback controller without considering the effect of hysteresis, and a PID feedback controller integrated with the feedforward hysteretic compensator.

요 약

이 논문에서는 압전작동기를 이용하여 유연 보 구조물의 위치추적제어를 실험적으로 고찰하였다. 작동기의 히스테리시스 특성을 보상하기 위한 앞먹임 보상기와 PID 되먹임 제어기를 함께 구성하여 정밀한 위치추적제어를 수행할 수 있도록 하였다. 히스테리시스 보상기는 압전작동기의 예측 변위를 바탕으로 한 프라이작 모델을 사용하여 구성하였다. 히스테리시스 보상기의 유무에 따른 PID 되먹임 제어의 성능을 조화가진과 랜덤 가진 실험을 통하여 평가하였으며, 보상기와 되먹임 제어기를 함께 사용하였을 때, 우수한 위치추적제어 성능을 가지는 것을 확인하였다.

1. 서 론

A smart structure is the one included to smart materials to perform sensing, control, and actuation. It possesses the outstanding characteristics such as high resolution and fast response. So, they are being applied increasingly in many fields such as micro-positioning[1~3], vibration suppression[4]. However, the high nonlinearity of the included smart materials limits the accuracy as well as the scope of applications. Hysteresis in piezoceramic materials is a kind of high nonlinearity. The response

† 교신저자; 정회원, 인하대학교 기계공학부
E-mail : seungbok@inha.ac.kr
Tel : (032)860-7319, Fax : (032)868-1716
* 인하대학교 대학원 기계공학과

of the piezoceramic to a voltage input is impossible to be predicted exactly unless the effect of hysteresis is considered. Therefore, in order to gain a high performance in control, the hysteresis has to be considered. Its effect has to be reduced or eliminated.

The main contribution of this work is to develop the compensator for hysteresis of the piezoactuator and incorporate with the flexible beam structure in order to achieve an accurate position tracking control of tip displacement. The hysteretic compensator is designed on the basis of Preisach model. In Preisach model, the main reversal curve and the first order ascending curves for numerical implementation are used to get a limit triangle database. On the other hand, the flexible beam is modeled using finite element method to obtain modal parameters such as natural frequency. Then, the position tracking control of a flexible piezoelectric beam is accomplished by using a PID feedback controller combined with the feedforward hysteretic compensator. Performance comparison between without and with the hysteretic compensator is made via experimental realization.

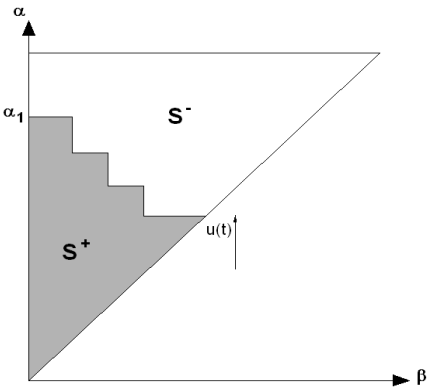

Fig. 1 The $\alpha\beta$ plane in the case of monotonically increasing of excitation voltage

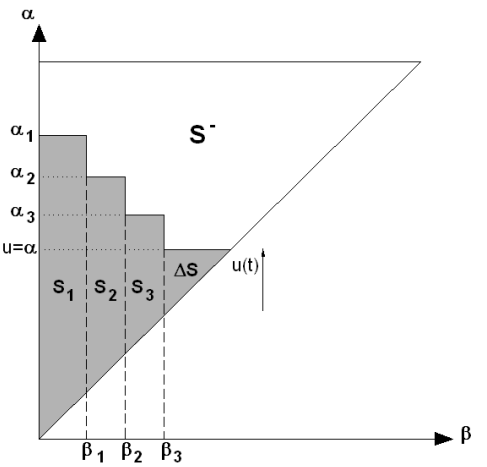

Fig. 2 The sub-regions constitute S^+

2. Modeling of Piezoactuator Hysteresis

The Preisach model can be numerically implemented by two approaches[5]; the first is to use the following formula for the computation of the input.

$$u(\alpha_1,\beta_1) = -\frac{\partial^2 Y(\alpha_1,\beta_1)}{\partial\alpha\partial\beta} \tag{1}$$

where, $Y(\alpha_1,\beta_1)$ is the change in output $y(t)$ as the input decreases from α_1 to β_1. Although this approach is straightforward, it encounters the main difficulty that the double numerical differentiation of experimentally obtained data may amplify errors seriously. Therefore, the second approach, the numerical implementation of the Preisach model, is preferable. It circumvents the above difficulty. This approach is based on the data collected from the main ascending curve and the first order reversal curves[5~7].

In our work, instead of using the data collected from the main ascending curve and the first order reversal curves, we use the data collected from the main reversal curve and the first order ascending curves for numerical implementation of the Preisach model. For the case of monotonically increasing of excitation voltage, at the time t_n, the corresponding $\alpha\beta$ plane is shown in Fig. 1.

The expansion of the piezoceramic can be expressed as follows.

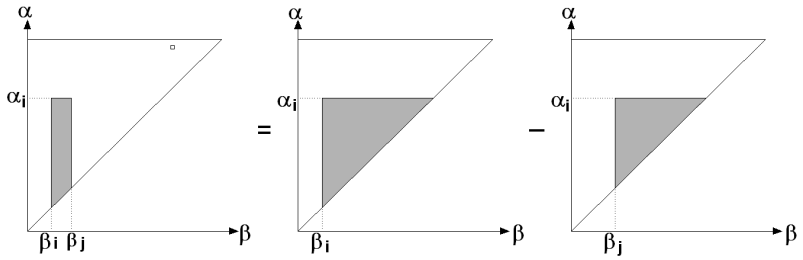

Fig. 3 The geometric calculation of $H(S_i^+)$

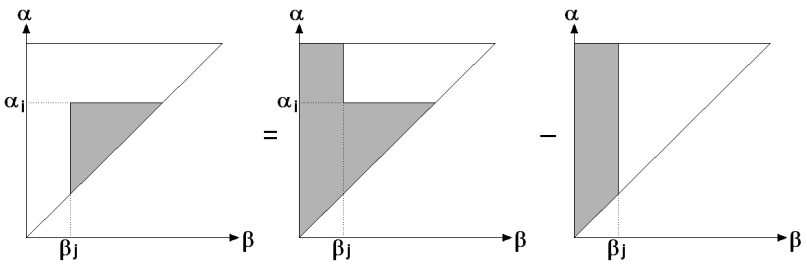

Fig. 4 The geometric calculation of $F(\beta_i,\alpha_j)$

$$y_{Pre}(u(t_n))=y_{ex}(m)+\iint_{\Delta s}\mu(\alpha,\beta)d\alpha d\beta \tag{2}$$

where, $y_{ex}(m)$ is the expansion of the piezo-ceramic at the nearest pair of extrema(include one maximum and one minimum). We assume that there are three pairs of extrema$(\alpha_i,\beta_i)i$=1,2,3. Therefore, $S^+(t_n)$ is subdivided into sub-regions as shown in Fig. 2.

The expansion of the piezoceramic actuator is given as

$$y_{ex}(3)=H(S_3^+)+H(S_2^+)+H(S_1^+) \tag{3}$$

where, from the outputs corresponding regions $S_i^+(i=1,2,3)$ shown in Fig. 3, the following mathematical expressions can be obtained.

$$H(S_3^+)=F(\beta_2,\alpha_3)-F(\beta_3,\alpha_3) \tag{4a}$$

$$H(S_2^+)=F(\beta_1,\alpha_2)-F(\beta_2,\alpha_2) \tag{4b}$$

$$H(S_1^+)=F(0,\alpha_1)-F(\beta_1,\alpha_1) \tag{4c}$$

where, $F(\beta_j,\alpha_i)$ is the value corresponding to the triangle limited by β_j and α_i. According to Fig. 4, this value can be expressed as follows.

$$F(\beta_j,\alpha_i)=g(\beta_i,\alpha_j)-g(\beta_i) \tag{5}$$

where, $g(\beta_i,\alpha_j)$ is the value at input α_j of first order ascending curve β_i; $g(\beta_i)$ is the value at the input β_i of main reversal curve. Substituting Eqs. (4) and (5) into Eq. (2) yields

$$y_{ex}(3)=g(\beta_3)+\sum_{k=1}^{3}\left[g(\beta_{k-1},\alpha_k)-g(\beta_k,\alpha_k)\right] \tag{6}$$

In general, with m pairs of extrema, one has the following form.

$$\begin{aligned} y_{ex}(m) &= g(\beta_m) \\ &\quad+\sum_{k=1}^{m}\left[g(\beta_{k-1},\alpha_k)-g(\beta_k,\alpha_k)\right] \end{aligned} \tag{7}$$

The second part of Eq. (2) is the value corresponding to the triangle limited by β_m and $u(t_n)$ and expressed as follows.

$$\begin{aligned} \iint_{\Delta S}\mu(\alpha,\beta)d\alpha d\beta &= F(\beta_m,u(t_n) \\ &= g(\beta_m,u(t_n))-g(\beta_m) \end{aligned} \tag{8}$$

Substituting Eq. (7) and (8) into Eq. (2) yields

$$y_{Pre}(u(t_n)) = g(\beta_m, u(t_n)) + \sum_{k=1}^{m} [g(\beta_{k-1}, \alpha_k) - g(\beta_k, \alpha_k)] \quad (9)$$

Similarly, for the case of monotonically decreasing of excitation voltage as shown in Fig. 5, an expression for expansion of piezoceramic actuator is developed as

$$y_{Pre}(u(t_n)) = g(\beta_2, \alpha_3) - g(u(t_n), \alpha_3) + \sum_{k=1}^{2} [g(\beta_{k-1}, \alpha_k) - g(\beta_k, \alpha_k)] \quad (10)$$

In general, with m pairs of extrema, we have the following form.

$$y_{Pre}(u(t_n)) = g(\beta_{m-1}, \alpha_m) - g(u(t_n), \alpha_m) + \sum_{k=1}^{m-1} [g(\beta_{k-1}, \alpha_k) - g(\beta_k, \alpha_k)] \quad (11)$$

Equations (9) and (11) give a numerical approach of Preisach model. In order to implement the model equation to determine the output to the input, a series of first-order reversal functions and a main ascending function for the piezoceramic actuator that are measured under static condition (i.e. the frequency of excitation voltage is fixed and set to be low) must be experimentally determined in advance. In our work, we use a series of first order ascending functions $g(\beta,\alpha)$ and a main reversal function $g(\beta)$ for the experiment database. This database is obtained by applying an input profile shown in Fig. 6.

The relationship between input and output consists of a series of first order ascending curve and a main reversal curve as shown in Fig. 7. The discretized values on the main ascending curve are $g(\beta)$, and the discretized values on the first order ascending curve are $g(\beta,\alpha)$.

In the case the point (β,α) does not lie on the grid point, it is determined by linear interpolation as follows.

$$g(\beta,\alpha) = c_0^{\beta\alpha} + c_1^{\beta\alpha}\beta + c_2^{\beta\alpha}\alpha + c_3^{\beta\alpha}\alpha\beta \quad (12)$$

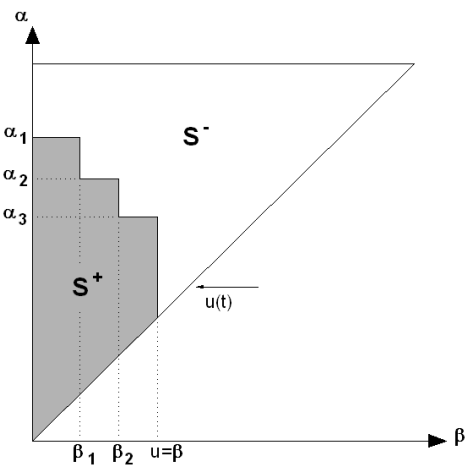

Fig. 5 The $\alpha\beta$ plane in the case of monotonically decreasing of excitation voltage

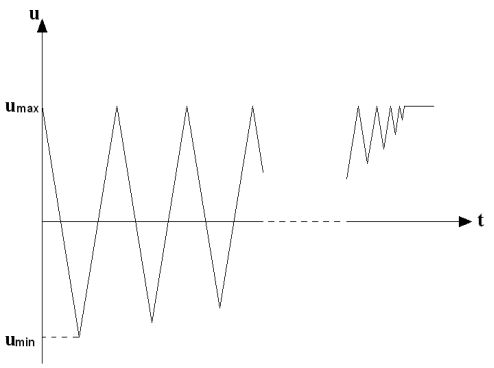

Fig. 6 The profile of the voltage input

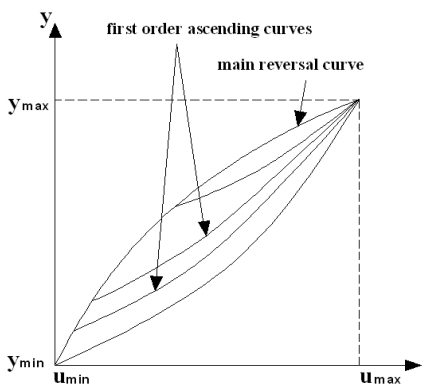

Fig. 7 Relationship between voltage and expansion

or

$$g(\beta,\alpha) = c_0^{\beta\alpha} + c_1^{\beta\alpha}\beta + c_2^{\beta\alpha}\alpha \tag{13}$$

Eq. (12) is used in the case the point (β,α) lies in a rectangle element, otherwise in the case the point (β,α) lies in a triangle element, Eq. (13) is used.

3. Design of Hysteretic Compensator

For the case of monotonically increasing of expansion $y_d(t_n) > y_d(t_{n-1})$, Eq. (9) can be written as

$$\begin{aligned} y_d(t_n) &= g(\beta_m, v(t_n)) \\ &\quad + \sum_{k=1}^{m} \left[g(\beta_{k-1},\alpha_k) - g(\beta_k,\alpha_k) \right] \end{aligned} \tag{14}$$

Substituting Eq. (12) into Eq. (14) yields

$$\begin{aligned} y_d(t_n) &= c_0^{\beta_m v(t_n)} + c_1^{\beta_m v(t_n)}\beta_m \\ &\quad + \left[c_2^{\beta_m v(t_n)} + c_3^{\beta_m v(t_n)}\beta_m \right] v(t_n) \\ &\quad + \sum_{k=1}^{m} \left[g(\beta_{k-1},\alpha_k) - g(\beta_k,\alpha_k) \right] \end{aligned} \tag{15}$$

Therefore, the expression for estimating $v(t_n)$ is obtained by

$$v(t_n) = \frac{y_d(t_n) - \left[c_0^{\beta_m v(t_n)} + c_1^{\beta_m v(t_n)} + \beta_m \right] - \sum_{k=1}^{m} \left[g(\beta_{k-1},\alpha_k) - g(\beta_k,\alpha_k) \right]}{\left[c_2^{\beta_m v(t_n)} + c_3^{\beta_m v(t_n)}\beta_m \right]} \tag{16}$$

Similarly, for the case of monotonically decreasing of expansion $y_d(t_n) < y_d(t_{n-1})$, the expression for estimating $v(t_n)$ is obtained by

$$v(t_n) = \frac{g(\beta_{m-1},\alpha_m) - y_d(t_n) - c_0^{v(t_n)\alpha_m} - c_1^{v(t_n)\alpha_m}\alpha_m + \sum_{k=1}^{m-1} \left[g(\beta_{k-1},\alpha_k) - g(\beta_k,\alpha_k) \right]}{\left[c_2^{v(t_n)\alpha_m} + c_3^{v(t_n)\alpha_m}\alpha_m \right]} \tag{17}$$

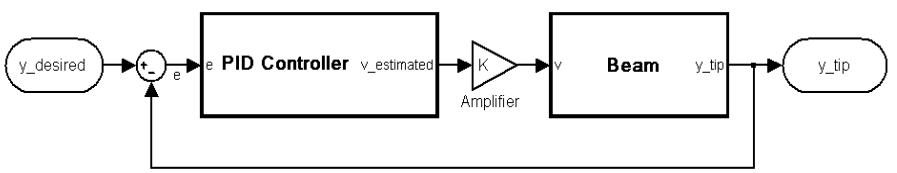

Fig. 9 The diagram block for discrete time PID tracking control without considering hysteretic behavior

4. Modeling of Flexible Beam

The schematic diagram of a composite beam is illustrated in Fig. 8. This beam consists of an aluminum beam bonded by a piezoceramic

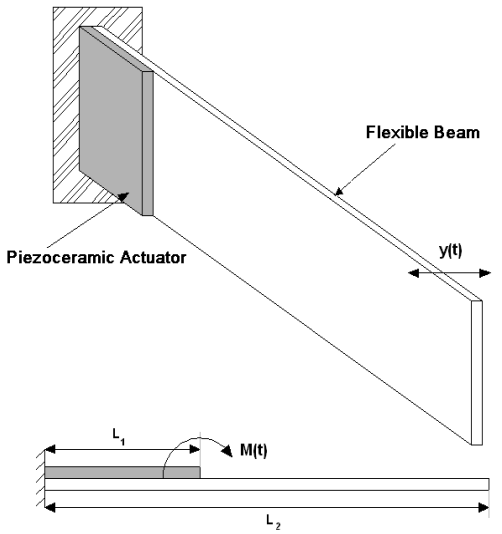

Fig. 8 The schematic diagram of the proposed flexible beam

actuator on one side of surface. In this section, the mathematical modeling of a beam based on Euler-Bernoulli beam theory and finite element method is adopted.

The element stiffness matrix can be derived as

$$\mathbf{K_e} = \frac{EI}{l^2}\begin{bmatrix} 12 & 6l & -12 & 6l \\ 6l & 4l^2 & -6l & 2l^2 \\ -12 & -6l & 12 & -6l \\ 6l & 2l^2 & -6l & 4l^2 \end{bmatrix} \tag{18}$$

The element mass matrix can be derived as

$$\mathbf{M_e} = \frac{ml}{420}\begin{bmatrix} 156 & 22l & 54 & -13l \\ 22l & 4l^2 & 13l & -3l^2 \\ 54 & 13l & 156 & -22l \\ -13l & -3l^2 & -22l & 4l^2 \end{bmatrix} \tag{19}$$

The mass and stiffness matrices of the entire beam are obtained by assembling the local mass and stiffness matrices using finite element method and combining the boundary conditions[8]. The governing equation of the beam in discretized form is given by

$$\mathbf{M}\ddot{\mathbf{Y}} + \mathbf{K}\mathbf{Y} = \mathbf{F}(t) \tag{20}$$

where, **Y** is the node displacement vector of the beam. **M** and **K** are respectively global mass and stiffness matrices. **F**(t) is the node force vector acting on the beam.

The dynamic response of Eq. (20) can be expressed as

$$\mathbf{Y}(t) = \sum_{r=1}^{N} \phi_r q_r(t) = \boldsymbol{\Phi}\mathbf{q}(t) \tag{21}$$

where, ϕ_r and $\mathbf{q}(t)$ are respectively the natural mode shape and generalized coordinate vectors.

Substituting Eq. (21) into Eq. (20) and pre-multiplying by ϕ_i^T give the following.

$$M_i\ddot{q}_i(t) + K_i q_i(t) = f_i(t) \tag{22}$$

where, $M_i = \phi_i^T\mathbf{M}\phi_i$; $K_i = \phi_i^T\mathbf{K}\phi_i$; $f_i(t) = \phi_i^T\mathbf{F}(t)$ Dividing by M_i and adding the damping term $2\xi_i\omega_i\dot{q}_i(t)$ Eq. (22) can be written as

$$\ddot{q}_i(t) + 2\xi_i\omega_i\dot{q}_i(t) + \omega_i^2 q_i(t) = \frac{f_i(t)}{M_i} \tag{23}$$

For simplicity, the first mode of vibration is only considered in this work. From Eq. (23), the first mode of vibration equation can be expressed as

$$\ddot{q}(t) + 2\xi\omega\dot{q}(t) + \omega^2 q(t) = \frac{f_1(t)}{M_1} \tag{24}$$

5. Experimental Results and Discussion

In order to verify the efficiency of the hysteretic compensator, two experimental approaches are carried out. Their qualities are evaluated and compared. These are “PID tracking control without feedforward hysteretic compensator” and “PID tracking control with feedforward compensator”. The parameters of PID controller in two approaches are similar.

PID tracking control without feedforward hysteretic compensator

In this approach, the relationship between the moment of the piezoceramic actuator and the voltage is considered to be linear[9].

$$M_p(t) = c.v(t) \tag{25}$$

where, c is the nominal (known) constant and dependent on material and geometrical properties of the beam. A discrete time PID controller can be expressed as follows[10].

$$v(k) = K_p\left\{e(k) + \frac{T}{T_I}\Sigma e(k) + \frac{T_D}{T}[e(k) - e(k-1)]\right\} \tag{26}$$

The diagram block for discrete time PID tracking control without considering hysteretic behavior is shown in Fig. 9. Fig. 10 and Fig. 11

show the tracking control response and tracking error curves respectively with a sine desired displacement. The average error is 1.752 μm Fig. 12 and Fig. 13 show the tracking control response and tracking error curves respectively with a random desired displacement. The average error is 1.405 μm.

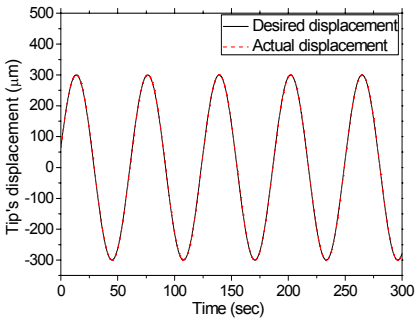

Fig. 10 Sine waveform displacement at the tip of the beam for discrete time PID tracking control without considering hysteretic behavior

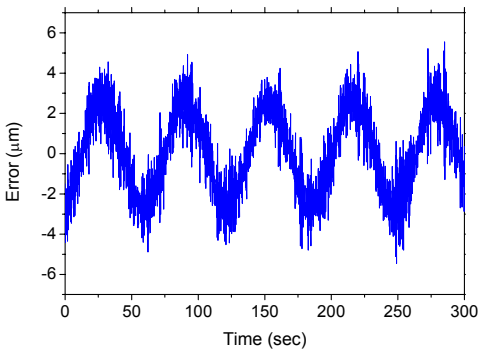

Fig. 11 The error curve between desired and actual sine waveform for discrete time PID tracking control without considering hysteretic behavior

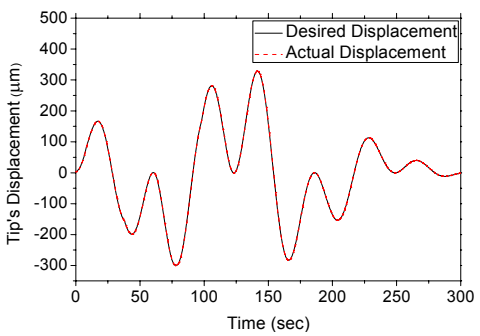

Fig. 12 Random waveform displacement at the tip of the beam for discrete time PID tracking control without considering hysteretic behavior

Clearly, the hysteresis of piezoceramic actuator, still limits the accuracy of PID controller. In theory, a linear controller such as a PID controller cannot eliminate completely the error of a nonlinear system. The greater rate of change of desired displacement is the larger error becomes.

PID tracking control with feedforward hysteretic compensator

In this control approach, the nonlinearity, hysteresis, is compensated separately. PID controller is then used to control the compensated system. The block diagram for discrete time PID tracking control with feedforward hysteretic compensator is shown in Fig. 14. Figure 15 and Fig. 16 show the tracking control response and tracking error curves respectively with a sine waveform input signal. The average error is 0.647. Figure 17 and Fig. 18 show the tracking control response and tracking error curves respectively with a random waveform input signal. The average error is 0.649 μm. As expected, the closed-loop PID tracking controller with the feedforward hysteretic

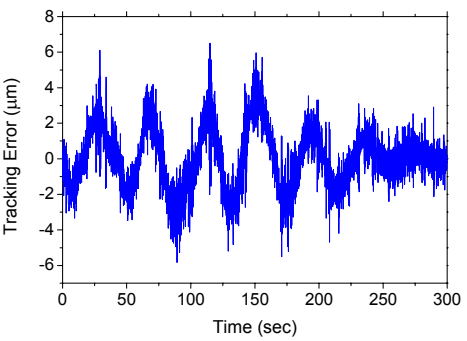

Fig. 13 The error curve between desired and actual random waveform for discrete time PID tracking control without considering hysteretic behavior

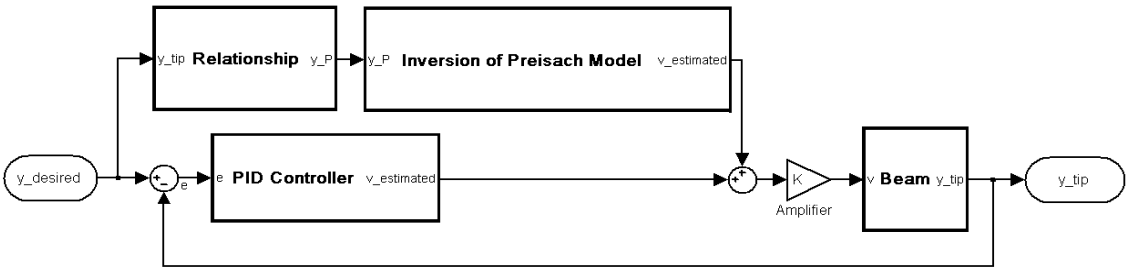

Fig. 14 The diagram block for discrete time PID tracking control with the feedforward hysteretic compensator

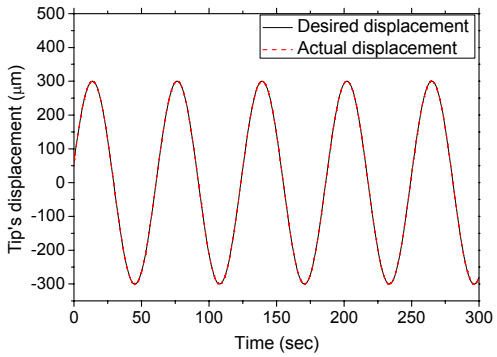

Fig. 15 Sine waveform displacement at the tip of the beam for discrete time PID tracking control with the feedforward hysteretic compensator

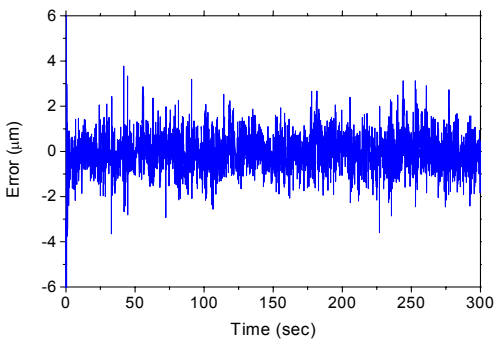

Fig. 16 The error curve between desired and actual sine waveform for discrete time PID tracking control with the feedforward hysteretic compensator

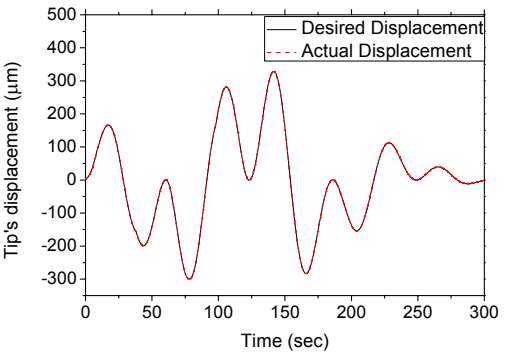

Fig. 17 Random waveform displacement at the tip of the beam for discrete time PID tracking control with the feedforward hysteretic compensator

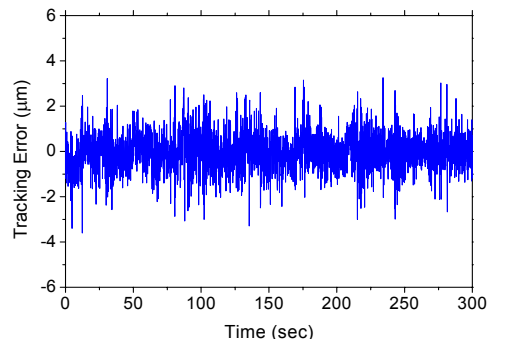

Fig. 18 The error curve between desired and actual random waveform for discrete time PID tracking control with the feedforward hysteretic compensator

compensator shows the smaller tracking error in comparison to the previous case. The error difference corresponding two desired displacements is not significant. The error profiles as shown in Fig. 16 and 18 become smoother compared with those in Fig. 11 and 13. Their values do not depend on the rate of change of the desired displacement any more. Moreover, they are more stable despite of the difference of desired

displacement forms. Clearly, the effect of hysteresis was eliminated significantly by the hysteretic compensator.

6. Conclusion

In this work, the position tracking control system of a flexible beam considering hysteresis behavior was conducted. In the system modeling, the flexible beam was modeled by finite element method and Preisach model was used for hysteretic compensator.

To implement the Preisach model, a set of first-order hysteretic ascending curves was measured. Higher order ascending curves were predicted based on experimental data and its effectiveness was experimentally verified. In order to increase the accuracy of the control system, a PID was used for feedback controller. For experiment, two control approaches were proposed and implemented. They are PID tracking control without hysteretic behavior and PID tracking control with the feedforward hysteretic compensator. It has been demonstrated through experimental implementation that PID tracking control with the feedforward hysteretic compensator has the better time and frequency tracking characteristics. It is finally remarked that in the near future the proposed control technique will be applied to more complicated systems such as position tracking control of a dual servo stage system.

Acknowledgement

This work was supported by the Ministry of Knowledge Economy(MKE) and Korea Industrial Technology Foundation(KOTEF) through the Human Resource Training Project for Strategic Technology.

References

(1) Furutani, K., Urushibata, M. and Mohri, N., 1998, “Displacement Control of Piezoelectric Element by Feedback of Induced Charge,” Nanotechnology. Vol. 9, No. 2, pp. 93~98.

(2) Shen, J. C., Jywe, W. J., Chiang, H. K. and Shu, Y. L., 2008, “Precision Tracking Control of a Piezoelectric-actuated System,” Precision Engineering. Vol. 32, No. 2, pp. 71~78.

(3) Ge, P. and Jouaneh, M., 1996, “Tracking Control of a Piezoceramic Actuator,” IEEE Transactions on Control Systems Technology, Vol. 4, No. 3, pp. 209~216.

(4) Choi, S. B. and Cheong, C. C., 1996, “Vibration Control of a Flexible Beam Using SMA Actuators,” Journal of Guidance, Control and Dynamics, Vol. 19, No. 5, pp. 1178~1180.

(5) Mayergoyz, I., 1991, “Mathematical Models of Hysteresis,” New York: Springer-Verlag.

(6) Ge, P. and Jouaneh, M., 1995, “Modeling Hysteresis in Piezoceramic Actuators,” Precision Engineering, Vol. 17, No. 3, pp. 211~221.

(7) Hu, H. and Ben, M. R., 2004, “A Discrete-time Compensation Algorithm for Hysteresis in Piezoceramic Actuators,” Mechanical Systems and Signal Processing, Vol. 18, No. 1, pp. 169~185.

(8) Seshu, P., 2004, “Textbook of Finite Element Analysis,” 1st ed. Prentice Hall of India, New Delhi.

(9) Baily, T. and Hubbard, J. E., 1985, “Distributed Piezoelectric Polymer Active Vibration Control of a Cantilever Beam,” Journal of Guidance, Dynamics and Control, Vol. 8, No. 5, pp. 605~611.

(10) Franklin, G. F., Powell J. D. and Workman M. L., 1992, “Digital Control of Dynamic Systems,” Addison-Wesley, Reading, MA.